Electronic Supplementary Information (ESI)

Three types of charged ligands based neutral phosphorescent iridium(III) complexes featuring nido-carborane: synthesis, structures, and solution processed organic light-emitting diode application

Qiuxia Li,[1] Chao Shi,[1*] Manli Huang,[2] Xinghua Zhang,[1] Fangxiang Sun,[3] Ying Zheng,[1] Hong Yan,[3*] Chuluo Yang[2*] and Aihua Yuan[1*]

Correspondence and requests for materials should be addressed to C.S. (shichao@just.edu.cn) or A.H.Y. (aihua.yuan@just.edu.cn) or C.L.Y. (clyang@szu.edu.cn) or H.Y. (hyan1965@nju.edu.cn)

Contents:

General information.....S2

Synthesis and characterization.....S2

X-ray crystal structure analysis.....S5

UV-vis absorption.....S8

OLED Device characterization.....S8

DFT calculation.....S9

^{1}H NMR spectra.....S11

References.....S13

General information

Unless noted, all reagents or solvents were obtained from commercial suppliers and used without further purification. All air sensitive experiments were performed in N_2 atmosphere through schlenk technology. Intermediate **1a**, **1b**, **2b**, **3b** and **4b** were synthesized according to literature procesures[1-4]. The ^{1}H and ^{11}B NMR spectra were measured by using a Bruker 400 MHz spectrometer at room temperature. Mass spectra were conducted at Micromass Q-Tof instrument (ESI) and Agilent Technologies 5973N (EI). A Hitachi F-4600 fluorescence spectrophotometer was used to measure phosphorescence spectral. An Edinburgh FLS-920 spectrometer was used to determine phosphorescence quantum efficiency and lifetimes of the molecules in solution. The experiments for cyclic voltametric were performed by using three electrode cell assemblies from an IM6ex instrument (Zahner). A one-compartment cell equipped with a platinum wire counter electrode, a Ag/Ag^{+} reference electrode, and a glassy-carbon working electrode was used for all measurements with a scan rate of 100 mVs^{-1}. The concentration of tetrabutylammonium hexafluorophosphate (Bu_4NPF_6) in dichloromethane solution a was 0.10 $molL^{-1}$ and used as supporting electrolyte.

Synthesis and characterization

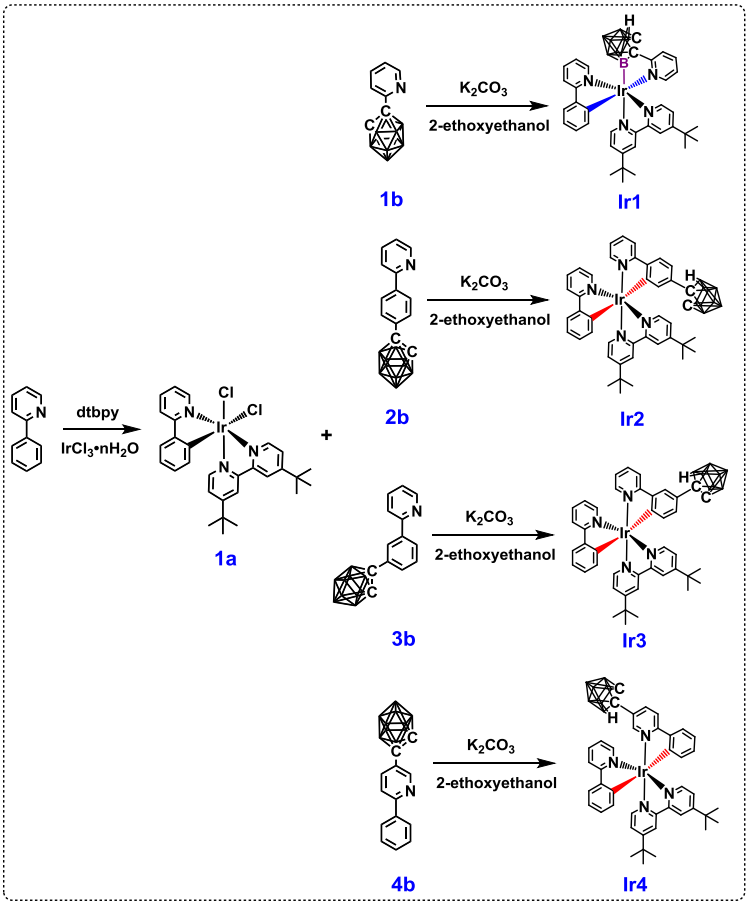

Fig. S1. The synthetic routes for three-charge (0, -1, -2) ligands based phosphorescent iridium(III) complexes (**Ir1**-**Ir4**) with different *nido*-carborane-containing dianionic (-2) ligands.

Synthesis and characterization of complexes

Synthesis and characterization of complex Ir1

1a (0.07 g, 0.1 mmol), 3b (0.02 g, 0.1 mmol) and K_2CO_3 (0.276 g, 0.2 mmol) were charged to a 100 mL schlenck tube, followed by 2-ethoxyethanol (15 mL). The mixture was heated to 150 ºC for 24 h under N_2. The resulting solution was dried and concentrated in vacuum, and target product was purified by column chromatography on silica gel with CH_2Cl_2 to afford yellow solid. 9.8 mg (24 %). ^{1}H NMR (400 MHz, CD_2Cl_2) δ 10.17 (d, *J* = 6.2 Hz, 1H), 8.13 (s, 1H), 8.01 (s, 1H), 7.91 (d, *J* = 8.2 Hz, 1H), 7.74 (t, *J* = 7.5 Hz, 1H), 7.60 (d, *J* = 5.6 Hz, 1H), 7.54 (d, *J* = 6.9 Hz, 2H), 7.44 (t, *J* = 6.8 Hz, 1H), 7.33 (d, *J* = 5.4 Hz, 1H), 7.01 (m, 2H), 6.89 (t, *J* = 6.2 Hz, 1H), 6.72 (m, 4H), 6.29 (d, *J* = 7.6 Hz, 1H), 4.07 (s, 1H, carborane), 1.39 (s, 9H), 1.33 (s, 9H), 0.34−2.22 (br, 8H, B−H), −3.13 (br, 1H, B−H−B). ^{13}C NMR (101 MHz, CD_2Cl_2) 176.3, 172.5, 169.8, 162.8, 161.2, 158.0, 156.8, 155.1, 153.8, 147.9, 147.3, 147.1, 144.5, 142.7, 137.5, 136.6, 130.6, 129.3, 125.3, 125.1, 124.5, 122.4, 122.1, 121.7, 120.4, 119.9, 119.8, 32.3, 30.5, 30.4, 29.7. ^{11}B NMR (CD_2Cl_2): −8.0 (2B), −12.1 (1B), −17.6 (3B), −26.6 (1B), −34.4 (2B). $C_{36}H_{46}IrB_9N_4$ calcd: C, 52.46; N, 6.80; H, 5.63. Found: C, 52.38; N, 6.76; H, 5.69. HR-MS: *m/z* calcd for $C_{36}H_{46}IrB_9N_4$ $[M]^+$: 826.4189.Found: 827.4261.

Synthesis and characterization of complex Ir2

1a (0.204 g, 0.3 mmol), 2b (0.18 g, 0.6 mmol) and K_2CO_3 (0.084 ml, 0.6 mmol) were charged to a 100 mL schlenck tube, followed by 2-ethoxyethanol (15 mL). The mixture was heated to 150 ºC for 24 h under N_2. The resulting solution was dried and concentrated in vacuum, and target product was purified by column chromatography on silica gel with CH_2Cl_2/petroleum ether 3: 1 (v/v) to afford yellow solid. 13.5 mg (5 %). ^{1}H NMR (400 MHz, CD_2Cl_2) δ 8.06 (m, 2H), 7.89 (m, 1H), 7.78 (m, 3H), 7.65 (m, 1H), 7.57 (m, 2H), 7.48 (m, 2H), 7.32 (m, 1H), 7.26 (m, 1H), 6.97(m, 5H), 6.75 (m, 1H), 6.52 (d, J = 7.1 Hz, 1H), 6.06 (dd, J = 6.6, 1.8 Hz, 1H), 3.57 (s, 1H, carborane), 1.38 (d, J = 3.5 Hz, 9H), 1.35 (d, J = 4.9 Hz, 9H), 0.32−2.50 (br, 9H, B−H), −2.72 (br, 1H, B−H−B). ^{13}C NMR (101 MHz, CD_2Cl_2) 170.6, 170.5, 170.1, 168.2, 162.4, 161.7, 156.1, 153.0, 152.8, 152.3, 147.7, 147.6, 144.8, 138.5, 138.3, 132.9, 132.8, 130.8, 129.5, 125.4, 124.3, 125.1, 124.3, 123.7, 123.6, 123.4, 122.3, 122.0, 121.9, 120.5, 120.4, 120.3, 119.9, 119.6, 31.2, 31.1, 29.9, 29.8. ^{11}B NMR (CD_2Cl_2): −9.5 (2B), −13.4 (1B), −16.0 (1B), −18.4 (1B), −23.0 (1B), −32.8 (1B), −35.7 (2B). $C_{42}H_{50}IrB_9N_4$ calcd: C, 56.03; N, 6.22; H, 5.60. Found: C, 55.96; N, 6.19; H, 5.63. HR-MS: *m/z* calcd for $C_{42}H_{50}IrB_9N_4$ $[M]^+$: 901.4539.Found: 901.4615.

Synthesis and characterization of complex Ir3

1a (0.204 g, 0.3 mmol), 3b (0.18 g, 0.6 mmol) and K_2CO_3 (0.084 ml, 0.6 mmol) were charged to a 100 mL schlenck tube, followed by 2-ethoxyethanol (15 mL). The mixture was heated to 150 ºC for 24 h under N_2. The resulting solution was dried and concentrated in vacuum, and target product was purified by column chromatography on silica gel with CH_2Cl_2/petroleum ether 3: 1 (v/v) to afford yellow solid. 27 mg (10 %). ^{1}H NMR (400 MHz, CD_2Cl_2) δ 8.03 (s, 2H), 7.92 (m, 3H), 7.79 (d, *J* = 5.6 Hz, 1H), 7.75 (d, *J* = 7.6 Hz, 1H), 7.65 (m, 3H), 7.49 (m, 2H), 7.24 (m, 2H), 7.07 (m, 1H), 6.98 (t, *J* = 7.1 Hz, 2H), 6.91 (t, *J* = 6.6 Hz, 1H), 6.79 (t, *J* = 6.6 Hz, 1H), 6.45 (d, *J* = 7.2 Hz, 1H), 6.20 (dd, *J* = 7.6, 2.1 Hz, 1H), 3.53 (s, 1H, carborane), 1.34 (s, 9H), 1.33 (s, 9H), 0.26−2.52 (br, 9H, B−H), −2.49 (br, 1H, B−H−B). ^{13}C NMR (101 MHz, CD_2Cl_2) 170.7, 170.4, 164.3, 161.7, 156.4, 155.9, 155.7, 153.0, 152.4, 147.7, 147.6, 146.2, 144.7, 141.5, 138.6, 138.5, 132.8, 131.6, 131.5, 130.9, 130.6, 129.9, 125.4, 125.2, 125.0, 123.7, 123.6, 123.5, 122.9, 120.4, 120.3, 120.2, 119.9, 35.4, 31.1, 29.9, 29.7. ^{11}B NMR (CD_2Cl_2): −9.7 (2B), −13.6 (1B), −18.4 (2B), −22.4 (1B), −32.8 (1B), −35.9 (2B). $C_{42}H_{50}IrB_9N_4$ calcd: C, 56.03; N, 6.22; H, 5.60. Found: C, 55.98; N, 6.18; H, 5.66. HR-MS: *m/z* calcd for $C_{42}H_{50}IrB_9N_4$ $[M]^+$: 901.4539.Found: 901.4626.

Synthesis and characterization of complex Ir4

1a (0.204 g, 0.3 mmol), 4b (0.18g, 0.6 mmol) and K_2CO_3 (0.084 ml, 0.6 mmol) were charged to a 100 mL schlenck tube, followed by 2-ethoxyethanol (15 mL). The mixture was heated to 150 ºC for 24 h under N_2. The resulting solution was dried and concentrated in vacuum, and target product was purified by column chromatography on silica gel with CH_2Cl_2/petroleum ether 3: 1 (v/v) to afford yellow solid. 54 mg (20 %). ^{1}H NMR (400 MHz, CD_2Cl_2) δ 8.05 (s, 2H), 7.92 (t, *J* = 7.5 Hz, 1H), 7.82 (m, 3H), 7.64 (m, 4H), 7.52 (m, 3H), 7.40 (m, 1H), 7.25 (m, 1H), 7.08 (m, 2H), 7.01 (t, *J* = 7.2 Hz, 1H), 6.92 (m, 1H), 6.45 (m, 2H), 3.54 (s, 1H, carborane), 1.35 (s, 9H), 1.34 (s, 9H), 0.28−2.63 (br, 9H, B−H), −2.76 (br, 1H, B−H−B). ^{13}C NMR (101 MHz, CD_2Cl_2) 169.8, 168.5, 164.6, 161.6, 156.1, 152.4, 150.1, 149.8, 147.9, 147.8, 147.7, 147.6, 147.4, 138.6, 136.2, 136.1, 132.7, 132.4, 131.8, 131.2, 129.9, 125.6, 125.2, 125.1, 124.7, 124.4, 123.9, 123.8, 123.5, 123.3 120.2, 118.9, 118.5, 95.9, 31.9, 31.1, 29.9, 29.3. ^{11}B NMR (CD_2Cl_2): −9.2 (2B), −13.3 (1B), −16.8 (2B), −19.7 (1B), −22.4 (1B), −32.5 (1B), −35.2 (1B). $C_{42}H_{50}IrB_9N_4$ calcd: C, 56.03; N, 6.22; H, 5.60. Found: C, 55.97; N, 6.17; H, 5.65. HR-MS: *m/z* calcd for $C_{42}H_{50}IrB_9N_4$ $[M]^+$: 901.4539.Found: 901.4606.

X-ray crystal structure analysis

Single-crystals of **Ir1**, **Ir2**, **Ir3** and **Ir4** were both obtained by slow diffusion of ethanol to their CH_2Cl_2 solutions, respectively. The X-ray diffraction data were collected on a Bruker Smart CCD Apex DUO diffractometer with graphite monochromated Mo Kα radiation (λ = 0.71073 Å) using the ω-2θ scan mode. All crystal datas are deposited in The Cambridge Crystallographic Data Centre (CCDC: 2094988 for **Ir1**, 2094989 for **Ir2**, 2094990 for **Ir3** and 2094991 for **Ir4**).

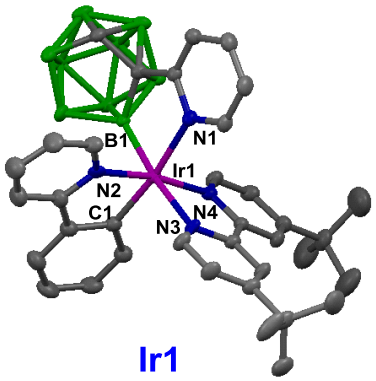

Fig. S2. Single crystal structure of **Ir1**, the hydrogen atoms have been omitted for clarity, selected bond lengths (Å) and angles (°): Ir1−N1 2.178(5), Ir1−B1 2.102(7), Ir1−C1 2.001(7), Ir1−N2 2.051(5), Ir1−N3 2.181(5), Ir1−N4 2.058(5); N1–Ir1–B1 80.2(2), N2–Ir1–C1 80.5(2), N3–Ir1–N4 77.0(2), B1–Ir1–C1 93.3(3), B1–Ir1–N2 84.4(2), B1–Ir1–N3 172.4(2), N2–Ir1–N4 170.3(2).

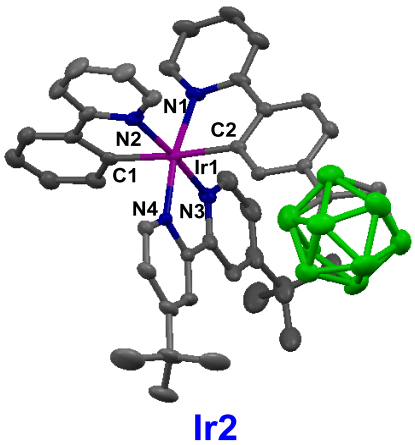

Fig. S3. Single crystal structure of **Ir2**, the hydrogen atoms have been omitted for clarity, selected bond lengths (Å) and angles (°): Ir1−N1 2.043(4), Ir1−C2 2.073(5), Ir1−C1 2.074(5), Ir1−N2 2.049(4), Ir1−N3 2.017(4), Ir1−N4 2.018(4); N1–Ir1–C2 79.73(18), N2–Ir1–C1 79.5(2), N3–Ir1–N4 79.51(18), C2–Ir1–N2 97.03(18), C2–Ir1–C1 175.1(2), C2–Ir1–N3 88.09(18), N2–Ir1–N3 174.29(17).

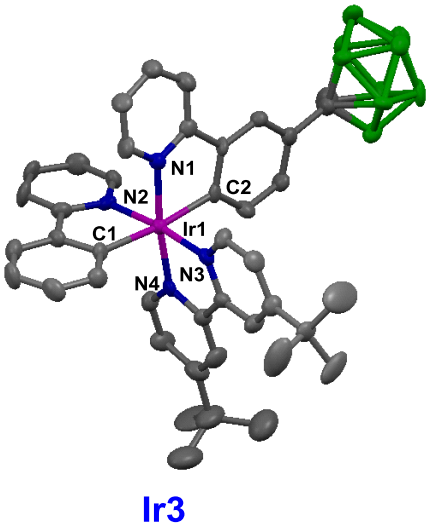

Fig. S4. Single crystal structure of **Ir3**, the hydrogen atoms have been omitted for clarity, selected bond lengths (Å) and angles (°): Ir1−N1 2.053(7), Ir1−C2 2.090(9), Ir1−C1 2.083(8), Ir1−N2 2.057(6), Ir1−N3 2.027(7), Ir1−N4 2.015(7); N1–Ir1–C2 96.0(3), N2–Ir1–C1 79.6(3), N3–Ir1–N4 79.1(3), C2–Ir1–N2 96.0(3), C2–Ir1–C1 173.5(3), C2–Ir1–N3 89.9(3), N2–Ir1–N3 172.8(3).

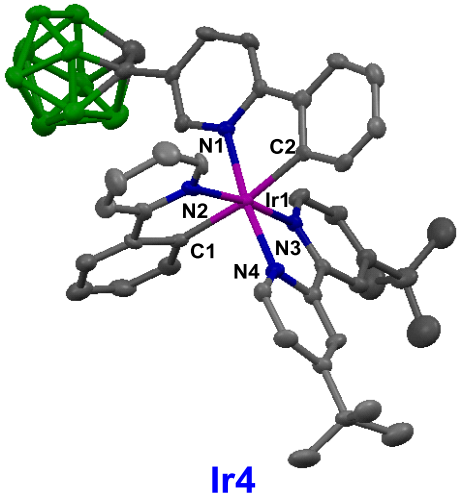

Fig. S5. Single crystal structure of **Ir4**, the hydroge atoms have been omitted for clarity, selected bond lengths (Å) and angles (°): Ir1−N1 2.054(8), Ir1−C2 2.050(9), Ir1−C1 2.091(11), Ir1−N2 2.069(10), Ir1−N3 2.037(8), Ir1−N4 2.048(9); N1–Ir1–C2 77.8(4), N2–Ir1–C1 80.0(4), N3–Ir1–N4 79.1(3), C2–Ir1–N2 95.1(4), C2–Ir1–C1 171.6(4), C2–Ir1–N3 91.1(3), N2–Ir1–N3 172.6(3).

Table S1. Crystallographic Data for three-charge (0, -1, -2) ligands based phosphorescent iridium complexes (**Ir1**-**Ir4**).

Complex	**Ir1**	**Ir2**	**Ir3**	**Ir4**
chemical formula	$C_{36}H_{46}B_9IrN_4 \cdot 3CHCl_3$	$C_{42}H_{50}B_9IrN_4$	$C_{42}H_{50}B_9IrN_4 \cdot 2CH_2Cl_2$	$C_{42}H_{50}B_9IrN_4$
formula weight	1182.38	900.37	1070.20	900.37
crystal size (mm)	0.17 ×0.18 × 0.22	0.33 × 0.37 × 0.40	0.04 × 0.11 × 0.17	0.30 × 0.34 × 0.36
temperature (K)	296	296	158	296
radiation	0.71073	0.71073	0.71073	0.71073
crystal system	Triclinic	Monoclinic	Triclinic	Triclinic
space group	P-1	P21/n	P-1	P-1
a(Å)	10.0398(7)	14.6519(7)	12.292(3)	10.867(6)
b(Å)	13.8768(9)	14.2649(7)	13.345(3)	15.625(9)
c(Å)	18.2289(12)	23.4999(12)	16.243(4)	15.643(9)
α(°)	97.701(1)	90	97.597(3)	80.335(9)
β(°)	91.015(1)	107.706(1)	91.556(3)	78.097(8)
γ(°)	98.251(1)	90	116.084(3)	88.512(9)
V(Å^3)	2488.9(3)	4679.0(4)	2361.2(10)	2562(3)
Z	2	4	2	2
ρ$_{(calc)}$ (g/cm^3)	1.578	1.278	1.505	1.167
F (000)	1172	1808	1072	904
absorp.coeff. (mm^{-1})	3.200	2.885	3.091	2.635
θ range (deg)	1.1 to 25.0	2.0 to 26.0	1.9 to 25.6	1.3 to 25.0
reflns collected	18608 (R_{int} = 0.032)	35583 (R_{int} = 0.046)	30929 (R_{int} = 0.082)	18671 (R_{int} = 0.085)
indep. reflns	8615	9183	8747	8919
Refns obs. [$I > 2\sigma(I)$]	7914	7112	6891	6429
data/restr/paras	8615/0/569	9183/0/547	8747/0/705	8919/0/515
GOF	1.14	0.81	1.06	1.06
R_1/wR_2 [$I > 2\sigma(I)$]	0.0388/0.1109	0.0391/0.1063	0.0537/0.1167	0.0621/0.1588
R_1/wR_2 (all data)	0.0451/0.1332	0.0574/0.1176	0.0811/0.1321	0.0946/0.1952
larg peak and hole(e/Å^3)	1.38/–1.40	1.67/–1.01	0.81/–1.07	2.83/–1.50

UV−vis absorption

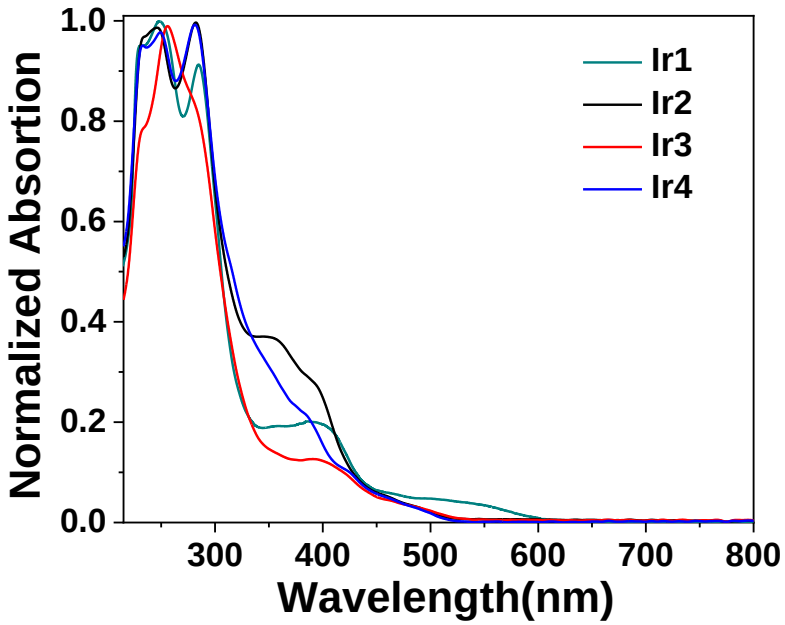

Fig. S6. UV/visible absorption spectra of three-charge (0, -1, -2) ligands based phosphorescent iridium complexes (**Ir1**-**Ir4**) in degassed CH_2Cl_2.

OLED Device characterization

The prepatterned indium tin oxide (ITO) substrates were cleaned by ultrasonic acetone bath, followed by ethanol bath. Afterwards, the substrates were dried with N_2 and then loaded into a UV-Ozone chamber. After UV-Ozone treatment, The PEDOT: PSS layer was spin-coated on the ITO substrate as the hole-injecting layer, and then annealed at 120 $^{\circ}$C for 10 min inside the N_2-filled glove-box. The emitter layer was also prepared by spin-coating directly on the hole-injecting layer, and then annealed at 50 $^{\circ}$C for 10 min. The electron-transporting material and the cathode material were thermally evaporated onto the emitter layer in a vacuum chamber. Before taken out of the glove-box, the devices were encapsulated with UV-curable epoxy. The voltage-current-luminance characteristics and the EL spectra were simultaneously measured with PR735 SpectraScan Photometer and Keithley 2400 sourcemeter unit under ambient atmosphere at room temperature.

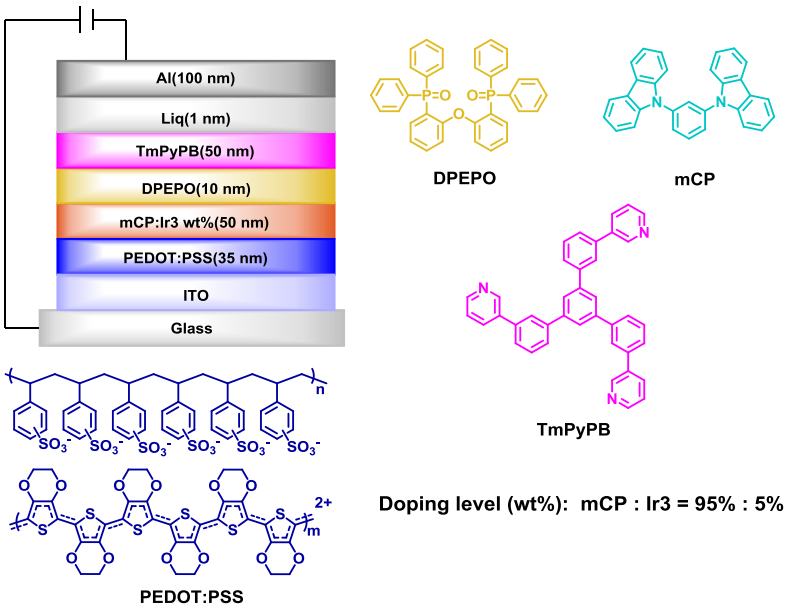

Fig. S7. Configuration of the OLEDs and chemical structures for the materials involved.

Table S3. EL performances of the device for **Ir3**.

complex	V_{on} [a] [V]	$EQE_{max}/CE_{max}/PE_{max}$ [b] [%/cd A^{-1}/lm W^{-1}]	λ_{ems} [c] [nm]	CIE [d] (x, y)
Ir3	6.4	2.6/3.3/9.0	558	(0.44, 0.52)

[a] Voltage in the luminance of 10 cd/m^2. [b] Maximum external quantum efficiency (EQE_{max}), maximum current efficiency (CE_{max}), maximum power efficiency (PE_{max}). [c] Maximum emission wavelength of the EL spectra. [d] The Commission Internationale de I'Eclairage (CIE) coordinates.

DFT calculation

DFT method was used to optimize the geometries all the complexes. The electronic transition energies and electron correlation effects were also calculated by (TD)-DFT method with the B3LYP functional (TD-B3LYP). The LANL2DZ basis set was used to treat with the iridium atom, and the 6–31G(d) basis set was used to treat with all other atoms. All calculations were carried out according to the Gaussian 09 program.[5]

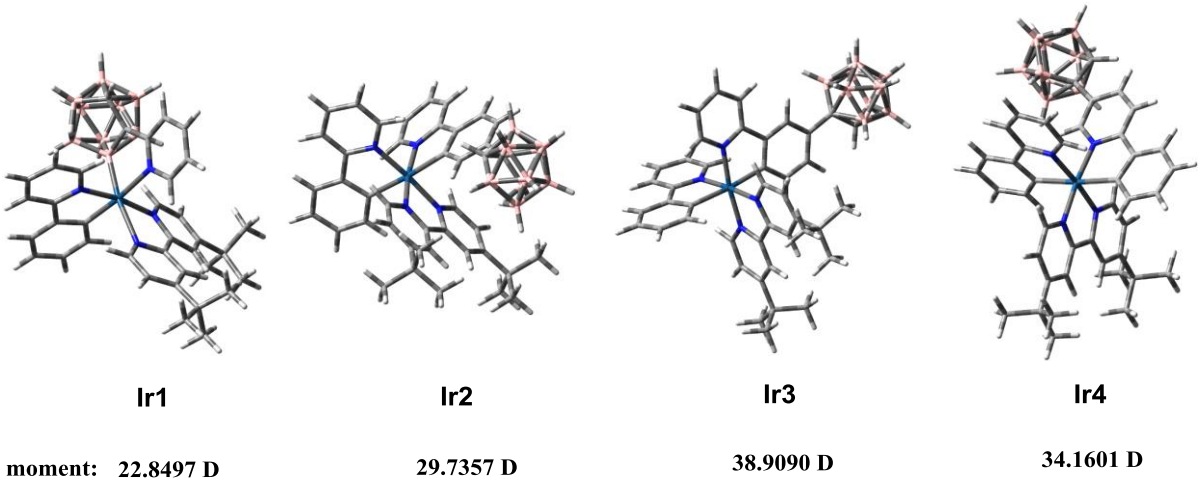

Fig. S8. Calculated structure and dipole moment of ground state for three-charge (0, -1, -2) ligands based phosphorescent iridium complexes (**Ir1**-**Ir4**).

Table S2. Calculated energies and oscillator strengths for lowest-energy singlet (S_1) and triplet (T_1) transitions.

complexes	states	E (eV)	Oscillator strength	main configurations (CI coeff)	Character
Ir1	S_1	1.66	0.0019	HOMO→LUMO (0.98)	LLCT/MLCT
	T_1	1.62	0	HOMO→LUMO (0.97)	^{3}LLCT/^{3}MLCT
Ir2	S_1	1.06	0.0001	HOMO→LUMO (0.99)	LLCT/LMCT
	T_1	1.06	0	HOMO→LUMO (0.99)	^{3}LLCT/^{3}LMCT
Ir3	S_1	0.62	0.0017	HOMO→LUMO (0.77)	LLCT/LMCT
	T_1	0.61	0	HOMO→LUMO (0.75)	^{3}LLCT/^{3}LMCT
Ir4	S_1	1.22	0	HOMO→LUMO (0.99)	LLCT/LMCT
	T_1	1.22	0	HOMO→LUMO (0.99)	^{3}LLCT/^{3}LMCT

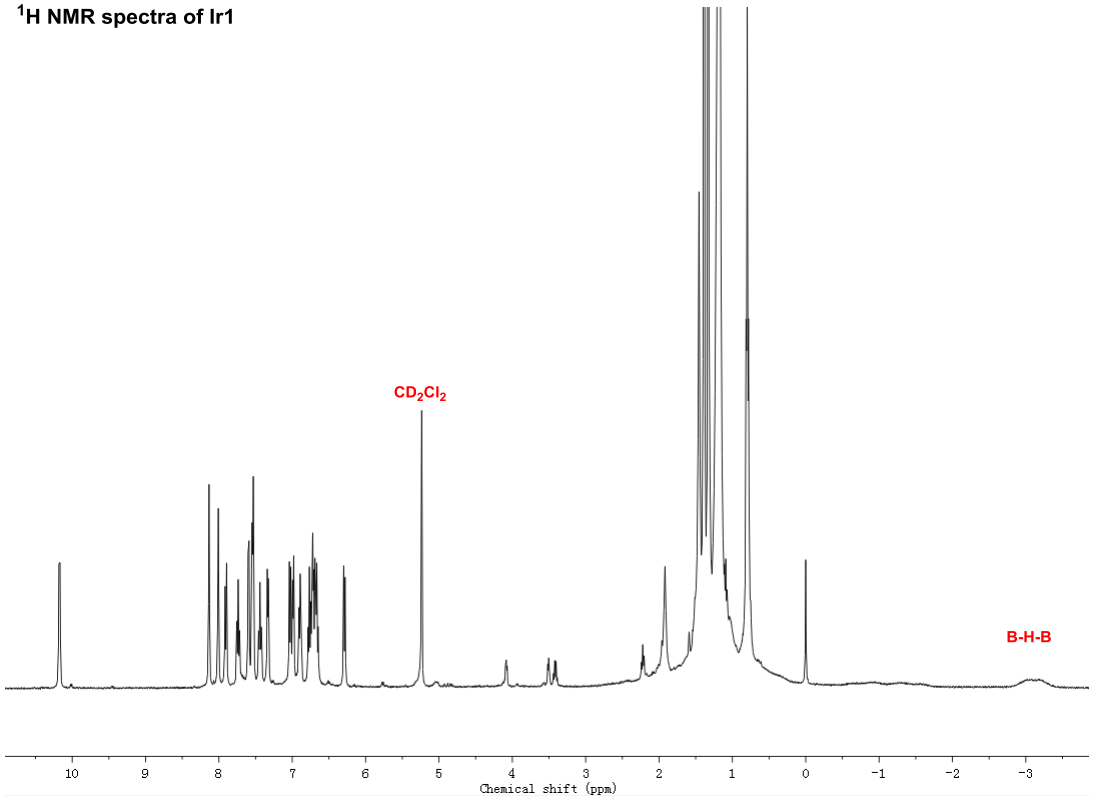

Fig. S9. ^{1}H NMR spectra of **Ir1**.

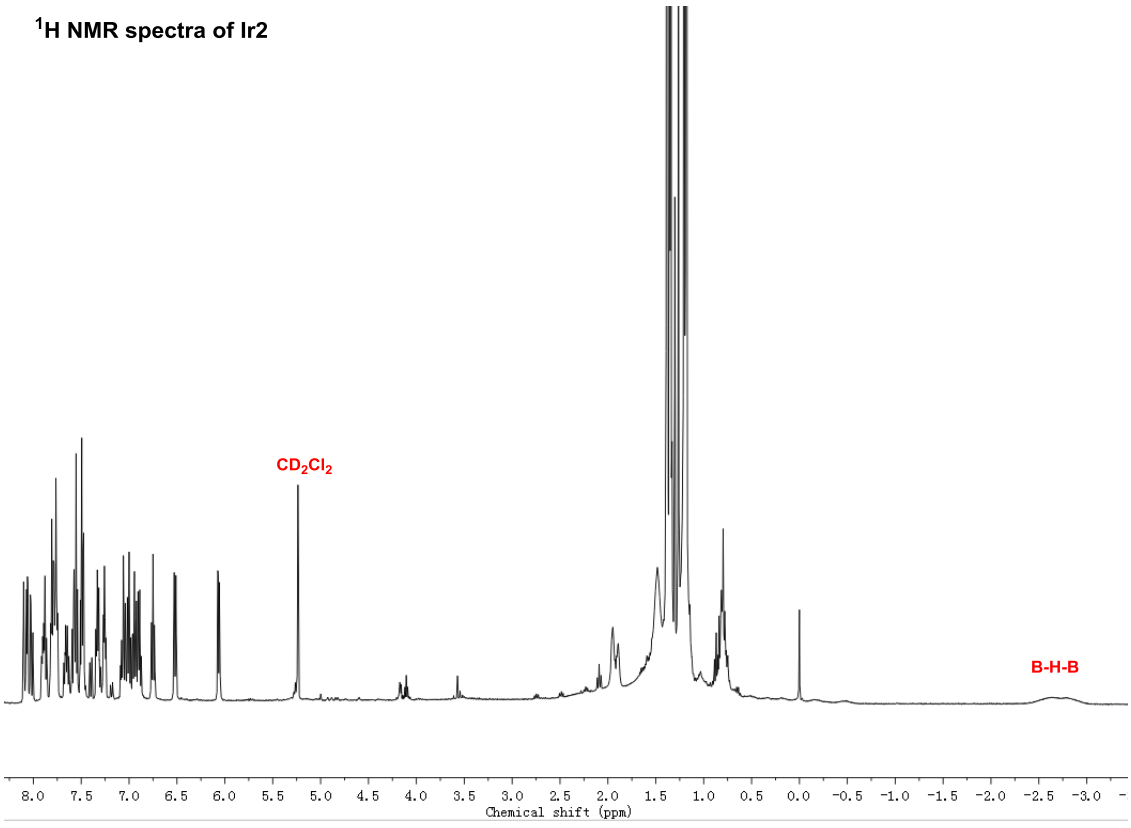

Fig. S10. ^{1}H NMR spectra of **Ir2**.

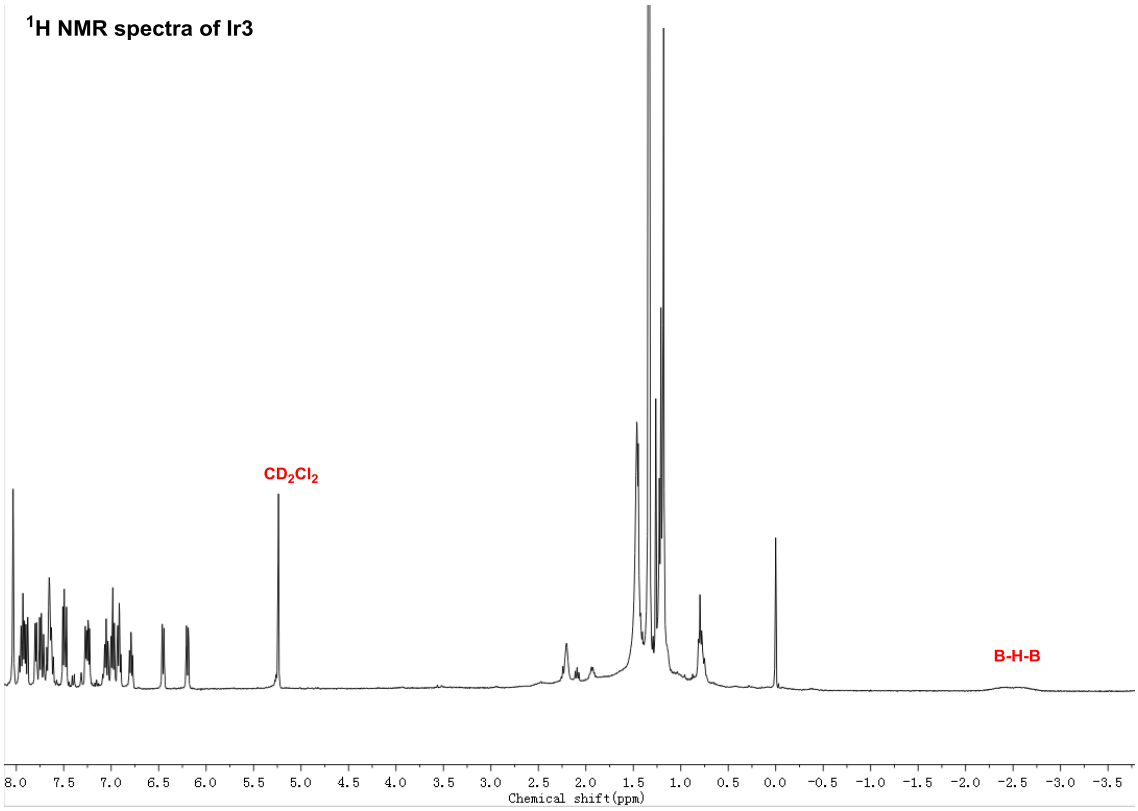

Fig. S11. ^{1}H NMR spectra of **Ir3**.

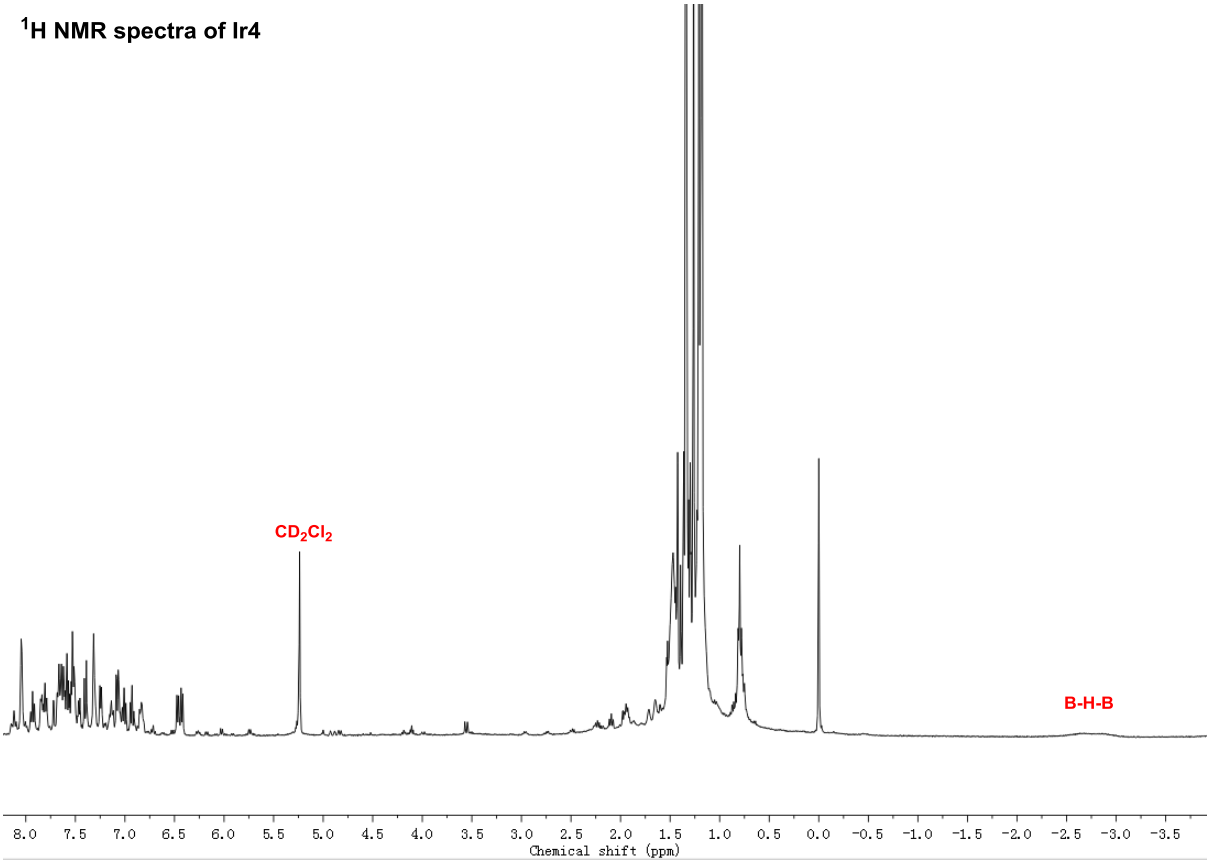

Fig. S12. ^{1}H NMR spectra of **Ir4**.

References

1. J. -L. Liao, Y. Chi, Z. -T. Sie, C. -H. Ku, C. -H. Chang, M. A. Fox, P. J. Low, M. -R. Tseng, G. -H. Lee, *Inorg. Chem.* 2015, **54**, 10811.
2. J. C. Axtell, K. O. Kirlikovali, P. I. Djurovich, D. Jung, V. T. Nguyen, B. Munekiyo, A. T. Royappa, A. L. Rheingold, A. M. Spokoyny, *J. Am. Chem. Soc.* 2016, **138**, 15758.
3. C. Shi, D. Tu, Q. Yu, H. Liang, Y. Liu, Z. Li, H. Yan, Q. Zhao, W. Huang, *Chem. Eur. J.* 2014, **20**, 16550.
4. X. Li, X. Tong, H. Yan, C. Lu, Q. Zhao, W. Huang, *Chem. Eur. J.* 2016, **22**, 17282.
5. M. J. Frisch, G. W. Trucks, H. B. Schlegel, G. E. Scuseria, M. A. Robb, J. R. Cheeseman, G. Scalmani, V. Barone, B. Mennucci, G. A. Petersson, H. Nakatsuji, M. Caricato, X. Li, H. P. Hratchian, A. F. Izmaylov, J. Bloino, G. Zheng, J. L. Sonnenberg, M. Hada, M. Ehara, K. Toyota, R. Fukuda, J. Hasegawa, M. Ishida, T. Nakajima, Y. Honda, O. Kitao, H. Nakai, T. Vreven, J. A. Montgomery Jr., J. E. Peralta, F. Ogliaro, M. Bearpark, J. J. Heyd, E. Brothers, K. N. Kudin, V. N. Staroverov, T. Keith, R. Kobayashi, J. Normand, K. Raghavachari, A. Rendell, J. C. Burant, S. S. Iyengar, J. Tomasi, M. Cossi, N. Rega, J. M. Millam, M. Klene, J. E. Knox, J. B. Cross, V.Bakken, C. Adamo, J. Jaram illo, R. Gomperts, R. E. Stratmann, O. Yazyev, A. J. Austin, R. Cammi, C. Pomelli, J. W. Ochterski, R. L. Martin, K. Morokuma, V. G. Zakrzewski, G. A. Voth, P. Salvador, J. J. Dannenberg, S. Dapprich, A. D. Daniels, O. Farkas, J. B. Foresman, J. V. Ortiz, J. Cioslowski and D. J. Fox, Gaussian 09, Revision B.01, Gaussian, Inc., Wallingford CT, **2010**.